

# Photocatalytic Degradation of Alizarin Red S and Bismarck Brown R Using TiO<sub>2</sub> Photocatalyst

## Research Article

Augustine Amalraj and Anitha Pius\*

Department of Chemistry, The Gandhigram Rural Institute - Deemed University, Dindigul - 624 302. Tamil Nadu, India

\*Corresponding author: Anitha Pius, Department of Chemistry, The Gandhigram Rural Institute - Deemed University, Dindigul - 624 302, India, Ph: +91-451-2452371 (O); Fax: +91-451-2454466 (O), E-mail: dranithapius@gmail.com

**Copyright:** © 2014 Pius A, et al. This is an open access article distributed under the Creative Commons Attribution License, which permits unrestricted use, distribution, and reproduction in any medium, provided the original work is properly cited.

**Article Information:** Submission: 30/07/2014; Accepted: 25/09/2014; Published: 27/09/2014

### Abstract

TiO<sub>2</sub> photocatalyst was prepared by the sol-gel method at a temperature of 300°C and characterized by SEM with EDS and FTIR. The photocatalytic degradation of Alizarin Red S (ARS) and Bismarck Brown R (BBR) was carried out using prepared TiO<sub>2</sub> photocatalyst irradiated with 16 W UV light source. The effect of various parameters, i.e., photocatalyst concentration, dye concentration, and pH of the solution on the percentage of degradation of selected dyes has been examined. The kinetic analysis of photodegradation of ARS and under different initial concentration followed the Langmuir-Hinshelwood model. TiO<sub>2</sub> can be an excellent photocatalyst candidate for the degradation of the selected dyes under UV light irradiation.

**Keywords:** TiO<sub>2</sub> nanoparticles; sol-gel method; Alizarin Red S; Bismarck Brown R; Langmuir-Hinshelwood model

### Introduction

Textile, paint, leather, detergent, paper, agrochemical and other industrial dyes constitute one of the largest groups of organic compounds that represent an increasing environmental risk. Over  $7 \times 10^5$  tons and above 10,000 different types of dyes and pigments are produced worldwide yearly. About 10-20% of the total world production of dyes is lost during dyeing process and is accordingly released in the textile wastewaters. The release of wastewaters that contain high concentration of dyes is a major trouble for the industry as well as a threat to the environment [1,2]. Dyes are extensively used in the textile industry, particularly those involved in finishing processes are among the major cause of water pollution. Due to the high concentration of organics in the effluents and the higher stability of modern synthetic dyes, these are not easily treated by chemical and biological methods and are released in wastewater. This is mainly due to the fact that dyestuffs are designed to be resistant to chemical loss and light induced fading. In addition, the stability of their molecular

structure also makes them resistant to aerobic microbial degradation [3].

Several physicochemical and biological methods currently exist for the treatment of dye industrial wastewaters. Physical methods basically do not degrade the pollutants but only transfer them from the liquid phase to the solid or another liquid phase, thereby causing secondary pollution [4]. Biological methods are more environmental friendly and easier to implement, but they have a major drawback of production of sludge and when the volume to treat is huge, recycling is necessary [5]. Furthermore, many of the dyes belong mostly to the non-biodegradable and unmanageable type of water pollutants [1,6]. Thus, there is a great challenge towards the treatment of textile effluents.

Therefore, new methods for the treatment of textile effluents, which should be cheaper and more efficient are being explored. Recently, the development of advanced oxidation processes in wastewater treatment research seems to complete these criteria. Heterogeneous

photocatalysis which employs only suitable semiconductor and light source appeared as a promising destructive technology leading to the complete removal of most of the pollutants [3,7,8]. Semiconductor materials employed in photoconversion systems present a moderately wide energy gap between the conduction band (CB) and the valence band (VB), this separation being known as the band-gap energy ( $E_{\text{gap}}$ ). The absorption of energy of certain wavelengths by a semiconductor promotes electron transfer from the VB to the CB, leaving vacancies in the VB called holes. The photogenerated electron/hole ( $e^-/h^+$ ) pair promotes the reduction and oxidation of species adsorbed at the surface of the semiconductor and induces oxidative degradation of species in solution through radical reactions [9,10].

Photocatalytic reaction using a semiconductor such as Titanium dioxide as photocatalyst is one of the advanced cost effective, clean and green technology which has attracted considerable interest for the termination of toxic organic and inorganic pollutants from wastewater [2,11]. The ability of this technique to completely degrade organics into water and carbon dioxide, without generating any harmful byproducts has popularized its role as a waste water purifier [2-12]. Titanium dioxide which is a metal oxide semiconductor is the most favored material in this technique, since it is chemically and biologically inactive, cheap, photostable and very photoactive, although it has a large energy gap (Eg) (3.2 eV) and only absorbs in the UV region.

Photocatalytic processes occur according to the following proposed mechanism: Irradiation of  $\text{TiO}_2$  particles with photons of energy equal to greater than the band gap energy ( $h\nu > E_{\text{g}}=3.2 \text{ eV}$ ;  $\lambda < 390 \text{ nm}$ ) results in the promotion of an electron from VB to the CB of the particle, The outcome of this process is the region of positive charge in the VB, termed as hole ( $h^+$ ) and a free electron ( $e^-$ ) in the CB (Eq. (1)):



The photo generated holes move around to the particle surface to react with the surface bound hydroxyl groups ( $\text{OH}^-$ ) and water molecules ( $\text{H}_2\text{O}$ ) to form hydroxyl ( $\text{OH}^\bullet$ ) radical (Eqs. (2) and (3)).



The photo generated electrons react with adsorbed molecular  $\text{O}_2$ , reducing it to superoxide radical anion  $\text{O}_2^{\bullet -}$  (Eq. (4)):



In the absence of an electron acceptor, most likely electron-hole recombination occurs. The presence of oxygen prevents recombination by catching electrons through the formation of superoxides ions, thereby protecting electron neutrality within the  $\text{TiO}_2$  molecule. The final product of the reduction is commonly hydroxyl radicals ( $\text{OH}^\bullet$ ). The hydroxyl radicals are known to be powerful oxidizing agents. During photocatalytic reactions, they can react with organic compounds and bacterial species adsorbed very close to the semiconductor surface, resulting in complete degradation into small inorganic species (Eqs. (5) and (6))



Dye stuffs from residual textile treatment water have been treated for the removal by this photodegradation technique [2, 13-18].

Alizarin Red S (ARS) and Bismarck Brown R (BBR) which are model compounds selected for this study, as they are water-soluble dyes and are used extensively as a coloring agent for fibers, leather, etc. [19-21]. The chemical structure of selected dyes ARS and BBR are shown in Figure 1. The wide use of this dye in industry and its water soluble nature maximize its chances of being present as a contaminant in industrial effluents. This study was conducted with the aim of preparing photocatalyst  $\text{TiO}_2$  nanoparticles by sol-gel method and examine the photodegradation kinetics of ARS and BBR. Degradation experiments were carried out with UV light/ $\text{TiO}_2$  at different illumination time,  $\text{TiO}_2$  doses, initial dye concentrations, and initial pH values in a photo reactor "Heber" photo reactor.

## Materials and methods

### Materials

Tetrabutyl titanate, ethanol Absolute AR (99.9%) and glacial acetic acid were purchased from Sigma Aldrich, India, were used for the preparation of  $\text{TiO}_2$ . Alizarin red S and Bismarck brown R of commercial grade were purchased from Nice chemicals Pvt. Ltd, Cochin, India. Hydrochloric acid and sodium hydroxide were also obtained from Sigma Aldrich India. All solutions and reaction mixtures were prepared in MilliQ water.

### Preparation of $\text{TiO}_2$ catalyst

The preparation of  $\text{TiO}_2$  nanophotocatalysts were carried out by sol-gel method. In this method, 20 mL tetrabutyl titanate and 4 mL acetic acid were added into 26 mL of absolute ethanol under continuous stirring condition to obtain solution A. 8 mL deionized water, 12 mL absolute ethanol and 12 mL acetic acid were mixed together to obtain solution B. Then, solution B was added drop wise into solution A under stirring. The obtained solution was sealed and stirring was continued for another 30 min at room temperature. The

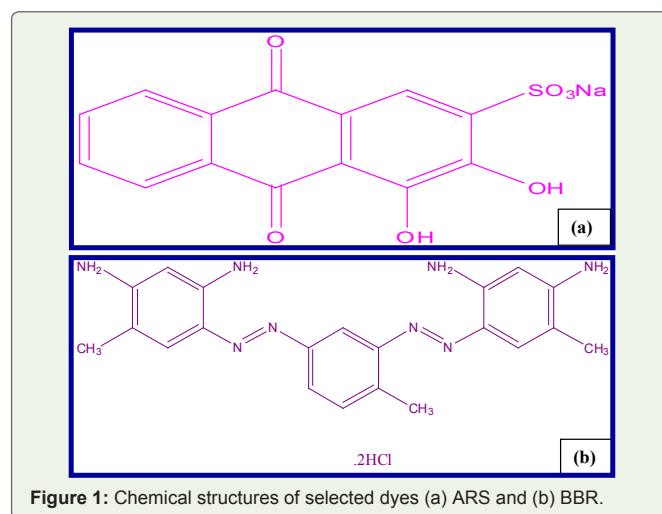


Figure 1: Chemical structures of selected dyes (a) ARS and (b) BBR.

resultant gel was aged at room temperature for 24 h and dried in an oven at 100°C for 36 h. After grinding, the gel was heat-treated in a furnace at 300°C for 3 h. and white crystalline TiO<sub>2</sub> nanoparticles were obtained at the end of the process [22].

### Characterization

The synthesized photocatalyst was characterized using scanning electron microscopy (SEM) with Energy Dispersive Spectrometry (EDS) analysis (Vega3Tescan, Bruker (Germany)). Infrared (IR) studies of TiO<sub>2</sub> were performed on a JASCO-460 plus FTIR spectrometer. UV-visible spectra of selected dyes were recorded using Perkin Elmer Lambda 35 (USA).

### Photodegradation of dyes under UV light in batch reactor

The photocatalytic degradation of ARS and BBR was performed in aqueous medium in a batch reactor. A cylindrical Pyrex glass photochemical reactor of 30 cm × 6 cm (height × diameter), provided with water circulation arrangement to maintain the temperature in the range 25-30°C, was used in all the experiments. The photodegradation was carried out using “Heber” photo reactor (16W, λ-max 251nm mercury lamp) placed inside a Pyrex glass jacket, thermostated by water circulation, and immersed in the dye solution contained in the batch reactor. The catalyst was maintained in suspension by stirring. Previously, the ARS and BBR solutions (50 ml, 50 mgL<sup>-1</sup>) containing 100 mg of photocatalyst were magnetically stirred in the presence of light for 60 min. Aliquots were withdrawn at specific time intervals and analyzed after filtration to remove the catalyst. The variation of the ARS and BBR dye concentrations as a function of irradiation time was determined using a UV-Visible spectrometer “Perkin Elmer Lambda 35” (USA) and the absorbance was measured at 517 nm and 465 nm against blank respectively

### Analytical methods

The concentration of the dyes ARS and BBR in the reaction mixture at different reaction time was monitored by UV spectrophotometry. The photodegradation efficiency of ARS and BBR was defined as follows:

$$\% = (C_0 - C_f) / C_0 \times 100 \quad (7)$$

Where C<sub>0</sub> is the initial concentration of dyes and C<sub>f</sub> is the concentration of dyes at certain reaction time *t* (min).

## Results and Discussion

### Characterization of prepared TiO<sub>2</sub> nanoparticles

SEM micrograph of prepared TiO<sub>2</sub> nanoparticles (Figure 2) shows that the material is formed by an agglomeration of nearly spherical particles having an average diameter of 60 nm. EDS analysis was used to characterize the elemental composition of the TiO<sub>2</sub> nanoparticles. A typical EDS pattern of TiO<sub>2</sub> nanoparticles is shown in Figure 3. Figure 4 shows the IR spectra of prepared TiO<sub>2</sub> nanoparticles. The broad band observed at 3431 cm<sup>-1</sup> is assigned to the asymmetrical and symmetrical stretching vibrations of hydroxyl group (-OH) and the band at 1627 cm<sup>-1</sup> is corresponds to deformative vibration of Ti-OH stretching modes. This band is an evidence of the adsorbed water on the TiO<sub>2</sub> surface [23,24]. The band at 1627 cm<sup>-1</sup> is assigned

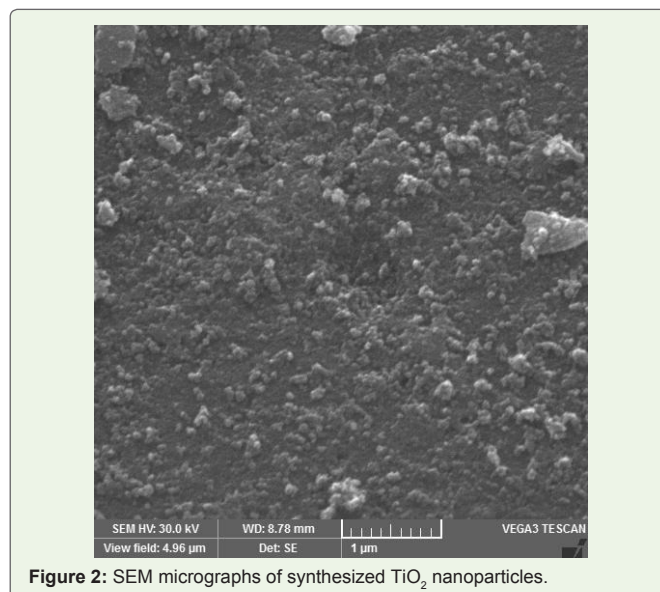


Figure 2: SEM micrographs of synthesized TiO<sub>2</sub> nanoparticles.

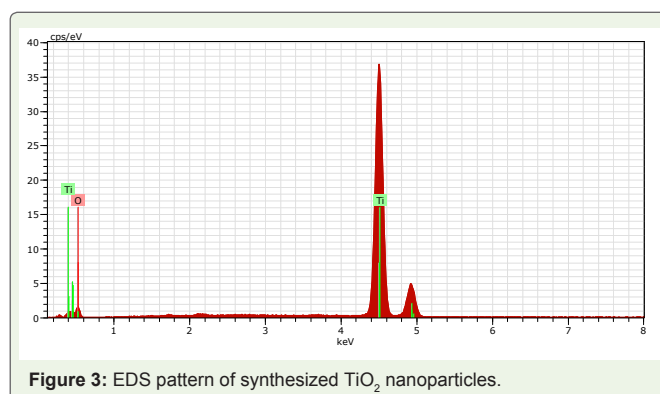


Figure 3: EDS pattern of synthesized TiO<sub>2</sub> nanoparticles.

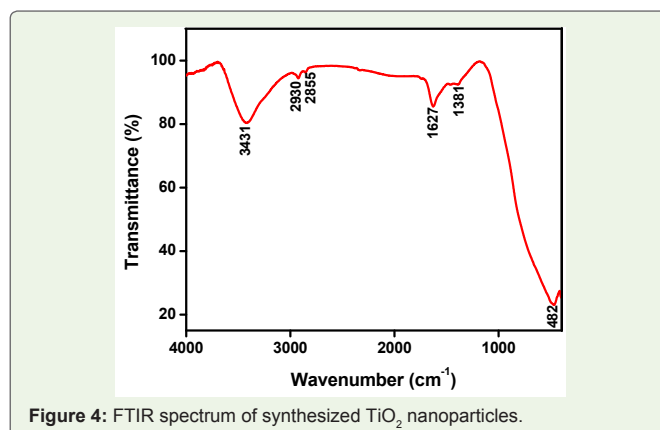


Figure 4: FTIR spectrum of synthesized TiO<sub>2</sub> nanoparticles.

to C=C bond which comes from the butyl groups after the sample was heat-treated at 300°C. The bands at 2930, 2855 cm<sup>-1</sup> and 1381 cm<sup>-1</sup> correspond to the stretching and bending modes of C-H bonds which come from the residual butyl group in the prepared TiO<sub>2</sub>. The band at 482 cm<sup>-1</sup> corresponds to the Ti-O bending mode of TiO<sub>2</sub> [22].

### UV-Visible Spectral Studies

Figure 5 shows the ultraviolet-visible (UV-Vis) spectrum of selected dyes ARS and BBR giving peaks at 517 nm and 465 nm against the blank respectively. The variation of ARS and BBR dye concentrations as a function of irradiation time was determined using a UV-Visible spectrometer.

### Effect of illumination time

The relationship between the photodegradation efficiency of ARS and BBR and the illumination time was investigated by fixing the amount of  $\text{TiO}_2$  as 100 mg. The result is shown in Figure 6. From the figure it can be seen that the photodegradation efficiency increased with the increase in the illumination time. The photodegradation of ARS and BBR increased from 19.2% to 94.1% and 10.0% to 91.4% respectively, when the illumination time increased from 10 to 80 min. The  $\text{OH}^\bullet$  is widely accepted as primary oxidants in heterogeneous photocatalysis. The oxidizing power of the  $\text{OH}^\bullet$  radicals is strong enough to completely oxidize dyes adsorbed on the surface of  $\text{TiO}_2$  into  $\text{CO}_2$ ,  $\text{H}_2\text{O}$  and other mineral acids as reported [25-27]. As seen in the Figure 6 when the illumination time was longer than 60 min, only small enhancement of photodegradation efficiency was observed. The probable reason is that, a large number of small organic molecules are produced by photodegradation with the increase of the irradiation time and these small organic molecules adsorb on the surface of  $\text{TiO}_2$ , resulting in the decreased formation of  $\text{OH}^\bullet$  radicals that attack the dyes, and therefore increase in illumination time does not lead to greater photodegradation efficiency of ARS and BBR.

### Effect of catalyst dose

The effect of photocatalyst dose on the degradation efficiency of ARS and BBR was investigated under UV light employing different dosages of  $\text{TiO}_2$  nanoparticles varying from 25 mg to 150 mg at a fixed dye concentration of  $10 \text{ mgL}^{-1}$ . The degradation efficiency of catalyst load on ARS and BBR is illustrated in Figure 7, which reveals that the efficiency increased greatly by increasing catalyst loading from 25 mg to 100 mg and thereafter the rate of degradation remains almost constant. Maximum degradation was observed with 100 mg dose of  $\text{TiO}_2$ . Similar results were obtained earlier by other workers [2,28]. The increase in the amount of catalyst increases the number of active sites on the  $\text{TiO}_2$  surface that in turn increases the number of  $\text{OH}^\bullet$  and  $\text{O}_2^{\bullet-}$  radicals [2,29]. Optimum catalyst loading found to be dependent on initial solute concentration. At the same time with high

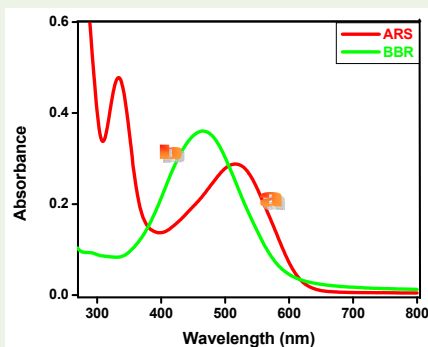


Figure 5: UV-vis spectra of the selected dyes (a) ARS and (b) BBR.

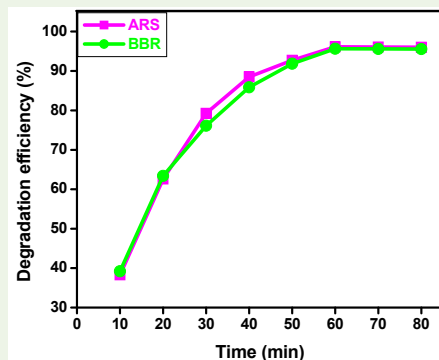


Figure 6: Effect of illumination time on the degradation of ARS and BBR dyes.

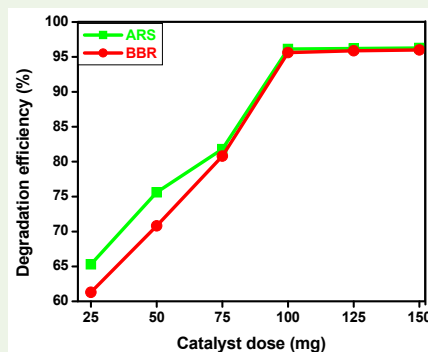


Figure 7: Effect of  $\text{TiO}_2$  dose on the degradation of ARS and BBR dyes.

dose of photocatalyst turbidity of the suspension increases, there will be a decrease in the penetration of UV light and hence photoactivated volume of suspension decreases [2,30]. Thus it can be concluded that a higher dose of catalyst may not be useful both in view of aggregation as well as reduced irradiation field due to light scattering. Therefore, catalyst dose of 100 mg was fixed for further studies.

### Effect of dye concentration

By varying the initial concentration from  $10$  to  $50 \text{ mgL}^{-1}$  at constant catalyst load (100 mg), its effect on the degradation rate was determined, and the results are shown in Figure 8. As seen in the figure, degradation efficiency of ARS and BBR decreased when increase the dyes concentration was increased. This negative result can be explained as follows; as the dye concentration is increased, the equilibrium adsorption of dye on the catalyst surface active sites increases; hence competitive adsorption of  $\text{OH}^\bullet$  on the same sites decreases, meaning a lower formation rate of  $\text{OH}^\bullet$  radical, which is the principal oxidant necessary for a high degradation efficiency. On the other hand, considering the Beer-Lambert law, as the initial dye concentration increases, the path length of photons entering the solution decreases, resulting in lower photon adsorption on catalyst particles and, consequently, a lower photodegradation rate.

### Effect of pH

An important parameter of photocatalytic reactions on the nano  $\text{TiO}_2$  surfaces is pH of the solution, since it states the surface charge

properties of the photocatalyst. The photodegradation efficiency of both ARS and BBR dyes was studied at different pH range from 3 to 11. The photodegradation efficiency of selected dyes as a function of reaction pH is shown in Figure 9. Photodegradation efficiency both of the dyes decreased with the increase in reaction pH and the highest efficiency was observed at pH 3. The explanation of pH effect on the photocatalytic process is very difficult because of its multiple roles, electrostatic interactions between the photocatalyst surface, solvent molecules, substrate and charged radicals formed during the reaction process [19,31]. The ionization state of the surface of the photocatalyst can be protonated and deprotonated under acidic and alkaline conditions respectively, as shown in the following equations,



The zero point charge (pzc) of the  $\text{TiO}_2$  is widely reported at  $\text{pH} \sim 6$  [29]. Thus,  $\text{TiO}_2$  surface will remain positively charged in acidic medium ( $\text{pH} < 6.25$ ) and negatively charged in alkaline medium ( $\text{pH} > 6.25$ ).

Higher uptakes of ARS obtained at lower pH values may be due to electrostatic attractions between ARS and more protonated adsorption sites available. A lower adsorption at higher pH values may be due to the abundance of  $\text{OH}^-$  ions and because of ionic repulsion between the negatively charged surface and the anionic ARS molecules [19]. The better efficiency for the degradation of BBR at lower pH may be due to the fact that the lone pairs of electrons present on the nitrogen atoms of amino groups can be protonated and deprotonated under acidic and basic conditions. Actually the photocatalytic oxidation seems to be favored in the structural orientation of the molecule, when it is protonated under lower pH values [31].

### Kinetic analysis

Photocatalytic degradation of ARS and BBR was performed in varying initial concentrations (10, 20, 30, 40 and 50  $\text{mg L}^{-1}$ ) for kinetic analysis. Heterogeneous photocatalysis process is very complicated, involving the function of many factors and even their mutual effect [32]. Figure 10 demonstrates the relationship between different initial concentrations of both ARS and BBR and time. It was found that

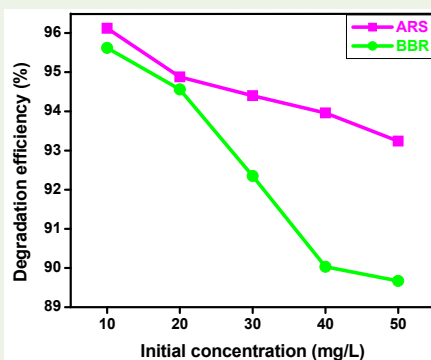


Figure 8: Effect of initial concentration on the degradation of ARS and BBR dyes.

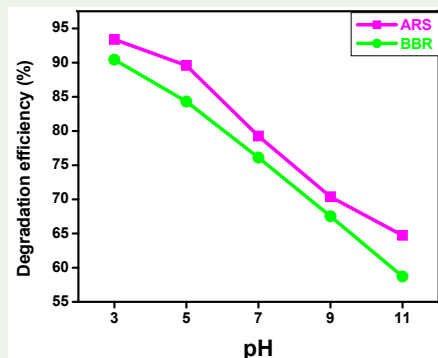
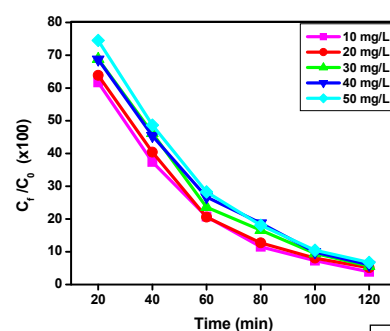
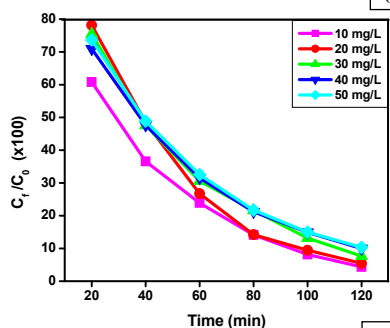


Figure 9: Effect of pH on the degradation of ARS and BBR dyes.



(a)



(b)

Figure 10: The relationship between different initial concentrations of (a) ARS and (b) BBR and time ( $\text{pH} 7.00$ ,  $\text{TiO}_2=100 \text{ mg}$ ).

photodegradation of ARS and BBR followed the pseudo first-order kinetic expression as can be seen from Figure 11. Table 1 shows the pseudo-first-order rate constant  $k_{\text{obs}}$ , and half-life  $t_{1/2}$  for photocatalytic degradation of ARS and BBR at different initial concentrations.

The influence of initial concentration of ARS and BBR on the photocatalytic degradation rate is described by pseudo-first order kinetic model for heterogeneous photocatalysis involving Langmuir-Hinshelwood expression [32-34]. The Langmuir-Hinshelwood model for dye degradation can be written as follows:

$$r = -\frac{d[\text{Dye}]}{dt} = k \frac{K_{\text{Dye}} [\text{Dye}]}{1 + K_{\text{Dye}} [\text{Dye}]_0} = k_{\text{obs}} [\text{Dye}] \quad (10)$$

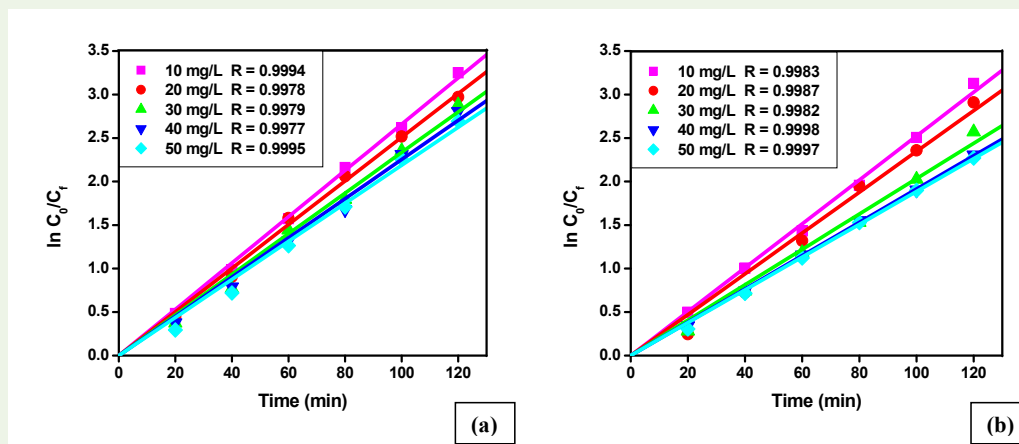


Figure 11: The relationship between  $\ln C_0/C_t$  and time at different initial concentrations of (a) ARS and (b) BBR.

Table 1: The values of the  $k_{obs}$  and half-lives of ARS and BBR under different initial concentrations.

Initial concentration of dyes ( $\text{mgL}^{-1}$ )	$k_{obs}$ ( $\text{min}^{-1}$ )		$t_{1/2}$ (min)		R	
	ARS	BBR	ARS	BBR	ARS	BBR
10	0.0266	0.0252	25.5844	13.2942	0.9994	0.9983
20	0.0251	0.0235	27.9933	14.2884	0.9978	0.9987
30	0.0234	0.0203	28.8610	16.1756	0.9979	0.9982
40	0.0225	0.0191	29.6371	18.0392	0.9977	0.9998
50	0.0219	0.0189	30.8795	18.3173	0.9995	0.9997

Table 2: values of the  $k$  and  $K_{Dye}$  of ARS and BBR.

Dyes	$k$ ( $\text{mgL}^{-1} \text{min}^{-1}$ )	$K_{Dye}$ ( $\text{Lmg}^{-1}$ )	R
ARS	4.8144	0.0058	0.9887
BBR	2.7463	0.01	0.9682

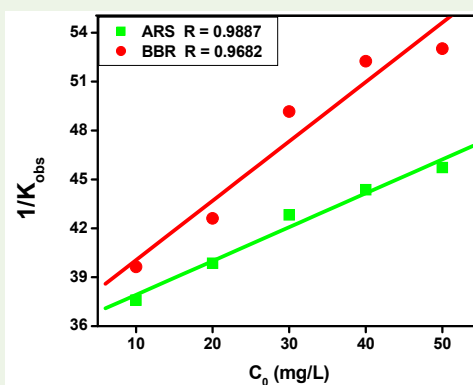


Figure 12: The relationship between  $1/k_{obs}$  and different initial concentrations of ARS and BBR.

$$\frac{1}{k_{obs}} = \frac{1}{kK_{Dye}} + \frac{[Dye]_0}{k} \quad (11)$$

where  $[Dye]_0$  is the initial concentration of dyes ( $\text{mgL}^{-1}$ ),  $K_{Dye}$  the Langmuir-Hinshelwood adsorption equilibrium constant ( $\text{Lmg}^{-1}$ ),  $k$  the rate constant of surface reaction ( $\text{mgL}^{-1}\text{min}^{-1}$ ), and  $k_{obs}$  pseudo-first-order rate constant. According to Eq. 11,  $1/k_{obs}$  holds a straight

line relation with the parameter  $[Dye]_0$ . When initial concentrations were plotted versus  $1/k_{obs}$ , the rate constant of surface reaction and the adsorption equilibrium constant were calculated (Table 2) to be  $k = 4.8144 \text{ mgL}^{-1} \text{ min}^{-1}$  for ARS and  $2.7463 \text{ mgL}^{-1} \text{ min}^{-1}$  for BBR and  $K_{Dye} = 0.0058 \text{ Lmg}^{-1}$  and  $0.01 \text{ Lmg}^{-1}$  for ARS and BBR respectively (Figure 12). The regression coefficient  $R$  was 0.9887 and 0.9682 for ARS and BBR respectively, which suggest the photodegradation of both dyes by the  $\text{TiO}_2$  fits the Langmuir-Hinshelwood kinetic expression well.

## Conclusions

TiO<sub>2</sub> photocatalyst can be efficiently applied for the degradation of Alizarin Red S and Bismarck Brown R dyes. Following conclusions are drawn from the results of the present study. The photocatalytic degradation process increased to some extent with increase in catalyst dose but decreased with increase in dye concentration. The maximum degradation was observed with 100 mg dose of TiO<sub>2</sub>. Photodegradation efficiency decreased with increase in reaction pH and the highest efficiency was observed at pH 3. The percentage of photodegradation of ARS was 94.1% and BBR was 91.4% when the solution was irradiated by the 16 W mercury lamp for 60 min. The kinetic analysis of photodegradation of ARS and BBR under different initial concentrations followed the Langmuir–Hinshelwood model. The rate constant of surface reaction and the adsorption equilibrium constants were calculated to be  $k = 4.8144 \text{ mgL}^{-1} \text{ min}^{-1}$  for ARS and  $2.7463 \text{ mgL}^{-1} \text{ min}^{-1}$  for BBR and  $K_{\text{Dye}} = 0.0058 \text{ Lmg}^{-1}$  and  $0.01 \text{ Lmg}^{-1}$  for ARS and BBR respectively. Prepared TiO<sub>2</sub> can be an excellent photocatalyst candidate for the degradation of the organic contaminants under UV light irradiation.

## References

- Juang RS, Lin SH, Hsueh PY (2010) Removal of binary azo dyes from water by UV-irradiated degradation in TiO<sub>2</sub> suspensions. *J Hazard Mater* 182: 820-826.
- Gupta VK, Jain R, Nayak A, Agarwal S, Shrivastava M (2011) Removal of the hazardous dye-Tartrazine by photodegradation on titanium dioxide surface. *Mat Sci Eng C* 31: 1062-1067.
- Zainal Z, Lee CY, Hussein MZ, Kassim A, Yusof NA (2007) Electrochemical-assisted photodegradation of mixed dye and textile effluents using TiO<sub>2</sub> thin films. *J Hazard Mater* 146: 73-80.
- Gupta AK, Pal A, Sahoo C (2006) Photocatalytic degradation of a mixture of crystal violet (basic violet 3) and methyl red dye in aqueous suspensions using Ag<sup>+</sup> doped TiO<sub>2</sub>. *Dyes Pigm* 69: 224-232.
- da Silva CG, Wang W, Faia JL (2006) Photocatalytic and photochemical degradation of mono-, di- and tri-azo dyes in aqueous solution under UV irradiation. *J Photochem Photobiol A: Chem* 181: 314-324.
- Petermel IT, Koprivanac N, Bozic AML, Kusic HM (2007) Comparative study of UV/TiO<sub>2</sub>, UV/ZnO and photo-Fenton processes for the organic reactive dye degradation in aqueous solution. *J Hazard Mater* 148: 477- 484.
- Hoffman MR, Martin ST, Choi WY, Bahnemann DW (1995) Environmental applications of semiconductor photocatalysis. *Chem Rev* 95: 69-96.
- Pozzo RL, Baltanas MA, Cassano AE (1997) Supported titanium oxide as photocatalyst in water decontamination: state of the art. *Catal Today* 39: 219-231.
- Zhao J, Chen C, Ma W (2005) Photocatalytic Degradation of Organic Pollutants Under Visible Light Irradiation. *Top Catal* 35: 269-278.
- de Souza ML, Corio P (2013) Effect of silver nanoparticles on TiO<sub>2</sub>-mediated photodegradation of Alizarin Red S. *Appl Catal B: Environ* 136-137: 325-333.
- Pruden AL, Ollis DF (1983) Photoassisted heterogeneous catalysis: the degradation of trichloroethylene in water. *J Catal* 82: 404-417.
- Legrini O, Oliveros E, Braun AM (1993) Photochemical processes for water treatment. *Chem Rev* 93: 671-698.
- Arslan I, Balcioglu IS, Bahnemann DW (2000) Advanced chemical oxidation of reactive dyes in simulated dye house effluents by ferrioxalate-Fenton/UV-A and TiO<sub>2</sub>/UV-A processes. *Dyes Pigm* 47: 207-218.
- Feng X, Zhu S, Hou H (2006) Photolytic degradation of organic azo dye in aqueous solution using Xe-excimer lamp. *Environ Technol* 27: 119-126.
- Hachem C, Bocquillon F, Zahraa O, Bouchy M (2001) Decolourization of textile industry wastewater by the photocatalytic degradation process. *Dyes Pigm* 49: 117-125.
- Saquib M, Muneer M (2003) Titanium dioxide mediated photocatalysed degradation of a textile dye derivative, acid orange 8, in aqueous suspensions. *Desalination* 155: 255-263.
- Saquib M, Muneer M (2003) TiO<sub>2</sub>-mediated photocatalytic degradation of a triphenylmethane dye (gentian violet), in aqueous suspensions. *Dyes Pigm* 56: 37-49.
- Ghaedi M, Hassanzadeh A, Nasiri Kokhdan S (2011) Multiwalled Carbon Nanotubes as Adsorbents for the Kinetic and Equilibrium Study of the Removal of Alizarin Red S and Morin. *J Chem Eng Data* 56: 2511-2520.
- Panizza M, Oturan MA (2011) Degradation of Alizarin Red by electro-Fenton process using a graphite-felt cathode. *Electrochim Acta* 56: 7084-7087.
- Ahmed S, Rasul MG, Wayde N, Martens, Brown R, Hashib MA (2011) Advances in Heterogeneous Photocatalytic Degradation of Phenols and Dyes in Wastewater: A Review. *Water Air Soil Pollut* 215: 3-29.
- Wang D, Xiao L, Luo Q, Li X, An J, Duan Y (2011) Highly efficient visible light TiO<sub>2</sub> photocatalyst prepared by sol-gel method at temperatures lower than 300°C. *J Hazard Mater* 192: 150-159.
- Zubieta CE, Messina PV, Schulz PC (2012) Photocatalytic degradation of acridine dyes using anatase and rutile TiO<sub>2</sub>. *J Environ Manage* 101: 1-6.
- Bezrodna T, Puchkovska G, Shymanosvska V, Baran J, Ratajczak H (2004) IR analysis of H-bonded H<sub>2</sub>O on the pure TiO<sub>2</sub> surface. *J Mol Struct* 700: 175-181.
- Wei L, Shifu C, Wei Z, Sujuan Z (2009) Titanium dioxide mediated photocatalytic degradation of methamidophos in aqueous phase. *J Hazard Mater* 164: 154-160.
- Houas A, Lachheb H, Ksibi M, Elaloui E, Guillard C, Herrmann JM (2001) Photocatalytic degradation pathway of methylene blue in water. *Appl Catal B: Environ* 31: 145-157.
- Chen CC, Lu CS, Chung YC, Jan JL (2007) UV light induced photodegradation of malachite green on TiO<sub>2</sub> nanoparticles. *J Hazard Mater* 141: 520-528.
- Muruganandham M, Swaminathan M (2006) Photocatalytic decolouration and degradation of Reactive Orange 4 by TiO<sub>2</sub>-UV process. *Dyes Pigm* 76: 133-142.
- Goncalves MST, Oliveira-Campos AMF, Pinto EMMS, Plasencia PMS, Queiroz MJRP (1999) Photochemical treatment of solutions of azo dyes containing TiO<sub>2</sub>. *Chemosphere* 39: 781-786.
- Daneshvar N, Khataee AR (2006) Removal of azo dye C.I. acid red from contaminated water using Fenton, UV/H<sub>2</sub>O<sub>2</sub>, UV/H<sub>2</sub>O<sub>2</sub>/Fe(II), UV/H<sub>2</sub>O<sub>2</sub>/Fe(III) and UV/H<sub>2</sub>O<sub>2</sub>/Fe(III)/oxalate processes: a comparative study. *J Environ Sci Health A* 41: 315-328.
- Abu Tariq M, Faisal M, Muneer M (2005) Semiconductor-mediated photocatalysed degradation of two selected azo dye derivatives, amaranth and Bismarck brown in aqueous suspension. *J Hazard Mater B127*: (2005) 172-179.
- Sun J, Wanga Y, Sun R, Dong S (2009) Photodegradation of azo dye Congo Red from aqueous solution by the WO<sub>3</sub>-TiO<sub>2</sub>/activated carbon (AC) photocatalyst under the UV irradiation. *Mater Chem Phys* 115: 303-308.
- De Heredia JB, Torregrosa J, Dominguez JR, Peres JA (2001) Oxidation of p-hydroxybenzoic acid by UV radiation and by TiO<sub>2</sub>/UV radiation: comparison and modelling of reaction kinetic. *J Hazard Mater* 83: 255-264.
- Chiou CS, Shie JL, Chang CY, Liu CC, Chang CT (2006) Degradation of di-n-butyl phthalate using photoreactor packed with TiO<sub>2</sub> immobilized on glass beads. *J Hazard Mater* 137: 1123-1129.